Theoretical Calculations of Coefficients of Friction between Weakly Interacting Surfaces

Nobuyuki N. Matsuzawa* and Noriyuki Kishii

SONY Corporation Research Center, 174 Fujitsuka-cho, Hodogaya-ku, Yokohama 240, Japan

Received: May 29, 1997; In Final Form: October 1, 1997[⊗]

Ab initio molecular orbital calculations were performed to predict the friction force and the coefficient of friction between surfaces contacted by van der Waals forces. Friction between graphite and a body terminated by hydrogen atoms was calculated for model systems of a naphthalene/hydrogen molecule and a pyrene/hydrogen molecule. The calculations showed that the friction for this system is isotropic. A coefficient of friction of 0.011−0.015 was predicted, which was in agreement with values from various friction-force microscope measurements, and was located at the lower limit of the macroscale experimental values. A theory to account for the calculated microscale friction is presented, and the derived results are compared to the calculated results.

1. Introduction

Friction occurs when two bodies in motion coming in contact with each other. Macroscopically, friction force F_f is known to be proportional to load F_N and the ratio of the two quantities gives the coefficient of friction μ as given in the following equation of Amontons' rule.[1,2]

$$F_f = F_N \times \mu \tag{1}$$

Because of the significance of the friction phenomena, much experimental and theoretical studies have been performed.[3−9] The AFM (atomic force microscope)[10,11] technology has been recently applied to friction phenomena, enabling measurements of the friction force at the atomic scale.[12−14] Using the AFM, several factors such as surface roughness and heterogeneity, which play an important role in macroscopic friction phenomena,[3−9] can at least partly be eliminated, giving us more idealized quantities than those from macroscopic measurements. Thus, a direct and quantitative comparison between numerical simulation and experimental values can be done for the friction at the atomic scale.

The total friction force (F_f) can be expressed as the sum of the molecular ($F_{f,ml}$) and mechanical ($F_{f,mc}$) friction force.[15]

$$F_f = F_{f,ml} + F_{f,mc} \tag{2}$$

Friction at the atomic scale may be represented by the first term in eq 2. Theoretical studies for the purpose of defining this term began with the independent oscillator model proposed by Tomlinson,[16] where energy dissipation during sliding without wear was formulated. This model consists of oscillators on the surface of a body (body A). The oscillators do not interact with each other, but interacting only with the other body (body B) which is moving in relative motion to body A. The model was modified by Frenkel and Kontorova,[17] to allow the presence of interaction between the oscillators on the surface of body A. These models suggest that for interfacial forces below a certain threshold size, frictionless slide occurs, whereas above the threshold, friction occurs with energy dissipation caused by the relaxation of the motion of the oscillators.[18]

Recent progress in computers has enabled us to perform numerical calculations of atomic-scale friction from the first principles. The first calculation was done by Zhong et al.,[19−21] and their model describes the friction which occurs above the threshold, i.e., in the region of strong interfacial interaction. The procedure that they applied can be regarded as one form of approximation of the oscillator model, where the relaxation energy of the oscillators is approximated by the energy difference between local maximum and minimum in the interbody potential surface. Their model was a four-layer slab of graphite and a monolayer of palladium, and the calculation method applied was local density functional theory with pseudopotentials. This model was chosen in order to simulate atomic-scale friction force measurements taken using an AFM,[12−14,22−29] where palladium in their model system corresponds to the tip of the AFM apparatus. It should be noted that the interfacial interaction present in their system may not only be attributed to the van der Waals force but also to the formation of chemisorption bonding[19−21] in the presence of metal/graphite interaction.

To obtain further insights into atomic-scale friction by applying first-principle theories, we calculated friction force and the coefficient of friction for contact of weakly interacting surfaces by applying the procedure described by Zhong et al.[19−21] Our model describes friction between graphite and a surface covered by hydrogen atoms, and ab initio molecular orbital (MO) theory was applied to calculate the van der Waals interaction with a better accuracy than the density functional theory. Referring to our calculated results, we also formulated the atomic-scale friction caused by the van der Waals interaction.

2. Calculations

To simulate atomic-scale friction between a graphite surface and a surface covered by hydrogen atoms, the model used should include as many atoms as possible. However, because of the computational time and memory involved, we chose naphthalene and pyrene as a model of the graphite surface and the hydrogen molecule as the model of the terminated hydrogen atoms, as shown in Figure 1.

The method of calculating friction force and the coefficient of friction used in this study is that proposed by Zhong et al.[19−21] If we designate the arrow in Figure 1 as the x axis, and the z axis as perpendicular to the plane of naphthalene or pyrene, the interaction potential between the hydrogen molecule and naphthalene or pyrene can be expressed as $E(x, z)$. The load f_N can then be given by the following equation.

* To whom correspondence should be addressed. E-mail address: nmatuzaw@src.sony.co.jp FAX number: +81-45-353-6909.

[⊗] Abstract published in *Advance ACS Abstracts,* November 15, 1997.

S1089-5639(97)01720-9 CCC: $14.00

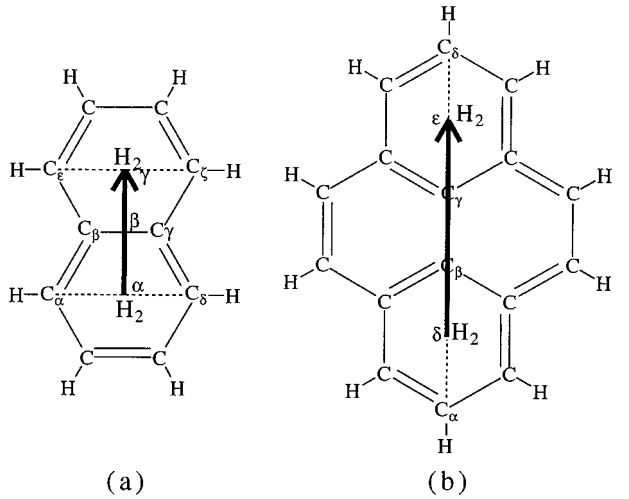

Figure 1. Model system for the calculation of the coefficient of friction. A hydrogen molecule moves over naphthalene or pyrene with its H−H bond being perpendicular to the molecules in this figure. The arrow shows the projected trajectory of the movement of the hydrogen molecule.

$$f_N = -\partial E(x, z)/\partial z \tag{3}$$

If load f_N is constant, the interaction potential under a constant load (isopressure potential, $E_f(x)$) can be expressed as:

$$E_f(x) = E(x, z_f) \tag{4}$$

where z_f is z under the condition given by eq 3.

Of course, this $E_f(x)$ is dependent on x. If we apply Zhong et al.'s procedure, the kinetic energy of the hydrogen molecule can be assumed to be consumed and dissipates when $\partial E_f(x)/\partial x > 0$, not returning to the hydrogen molecule when $\partial E_f(x)/\partial x < 0$.[9] Thus, the energy difference between a local minimum and maximum of $E_f(x)$ corresponds to the amount of energy to be dissipated, and by dividing this amount by the distance between the minimum and maximum, the friction force in the atomic scale (f_f) under load f_N can be obtained. The coefficient of friction μ is obtained by

$$\mu = f_f/f_N \tag{5}$$

To simulate atomic-scale friction, one must choose a path to move hydrogen over graphite to calculate $E(x, z)$. Strictly speaking, one needs to calculate friction force or the coefficient for all possible paths over graphite, and then the obtained values must somehow be averaged. However, this requires a significant computational time and memory at ab initio MO levels, so that we performed calculations only for two different paths, as shown in Figure 1. For both of the two paths in Figure 1, the hydrogen molecule moves from the center of a six-membered ring to the center of another six-membered ring. For these paths, computational time and memory can further be reduced because of the presence of symmetry, as compared to other paths which do not pass over the center of a six-membered ring. In Figure 1a, the hydrogen molecule moves over the center of a C−C bond (point β), whereas in Figure 1b, the molecule moves along a C−C bond, passing over carbon atoms of C_β and C_γ. The former case may be a path where the energy difference between maximum and minimum is the lowest under the restriction on path, whereas the latter case is the highest, if the load is around zero. Thus, calculations for these two paths may yield typical values for friction force and the coefficient for the graphite/hydrogen interface, which can be used to clarify the dependence of the quantities on the choice of path. It should be noted that the path in Figure 1a is the one also applied by Zhong et al., whereas the path in Figure 1b is not.[19−21]

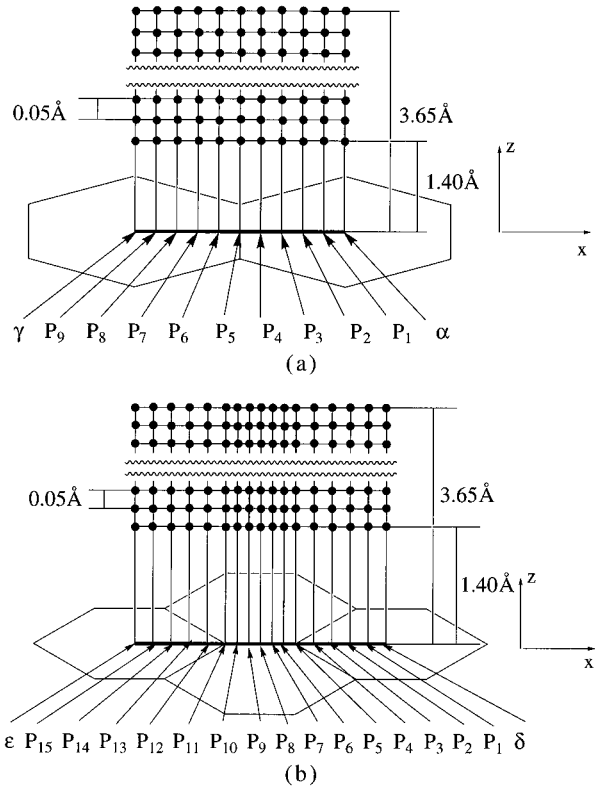

Figure 2. Grid points for the energy calculations. The hydrogen atom in the hydrogen molecule closer to naphthalene or pyrene than the other is located at the grid points with the H−H bond in the hydrogen molecule being perpendicular to the plane of naphthalene or pyrene. Definition of the designation of points is also shown.

In our model, the H−H bond of the hydrogen is perpendicular to the plane of naphthalene or pyrene. Thus, among the two hydrogen atoms in the hydrogen molecule, the one closer to naphthalene or pyrene corresponds to the terminated hydrogen atoms, and the other is present in order to eliminate a dangling bond which would be present if a hydrogen atom is used for the model instead of a hydrogen molecule.

Energy calculations were done using the program system Gaussian.[30] The basis sets used were 6-31G*[31−35] and 6-311G*[36,37] for the naphthalene/hydrogen system and 6-31G* for the pyrene/hydrogen system. The second-order Møller−Plesset perturbation theory[38] was applied as an electron-correlation treatment. Geometry optimizations of naphthalene, pyrene, and hydrogen were performed at the level corresponding to the energy calculations. The optimized geometries were then used for the energy calculations to obtain $E(x, z)$. All the calculations were done by using a Cray J916/12-4096 computer.

For calculating $E(x, z)$ along the paths, grid for the position of the hydrogen molecule must be constructed. The grids applied are shown in Figure 2, where points marked by filled circles in the figure correspond to the positions of the hydrogen atom in the hydrogen molecule closest to naphthalene or pyrene. As shown in Figure 2, the energy calculations were done for z (the distance from the line $\alpha-\gamma$ in Figure 1a[39] or the distance from the line $\delta-\epsilon$ in Figure 1b[40]), varying from 1.40 to 3.65 Å with an increment of 0.05 Å (and so yielding 46 points) both for the naphthalene/hydrogen and pyrene/hydrogen systems. For the x-axis, points to calculate the energies were those which divide the segment of the line $\alpha-\gamma$ (Figure 1a) equally into 10 for the naphthalene/hydrogen system ($\Delta x = 0.2483$ Å for MP-

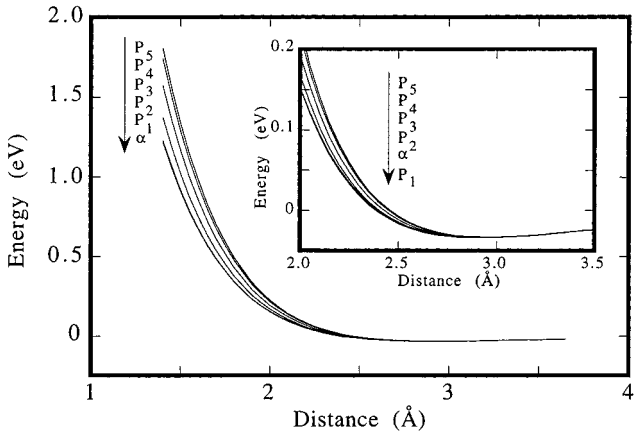

Figure 3. Intermolecular potentials for the naphthalene/hydrogen molecule system calculated at the MP-2/6-311G* level. Inset is a magnified figure for the range from 2.0 Å to 3.5 Å of the distance. The horizontal scale is the distance between the plane of the substrate molecule (naphthalene or pyrene) and the hydrogen atom closest to the substrate molecule in the hydrogen molecule.

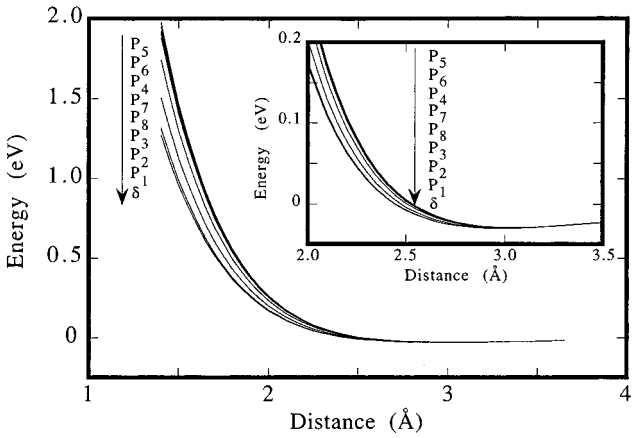

Figure 4. Intermolecular potentials for the pyrene/hydrogen molecule system calculated at the MP-2/6-31G* level. Inset is a magnified figure for the range from 2.0 Å to 3.5 Å of the distance. The horizontal scale is the distance between the plane of the substrate molecule (naphthalene or pyrene) and the hydrogen atom closest to the substrate molecule in the hydrogen molecule.

2/6-31G*, and $\Delta x = 0.2487$ Å for MP-2/6-311G*). For the *x*-axis in the system of pyrene/hydrogen, energies were calculated at points which divide the segment of the line δ-C_β and C_γ-ϵ equally into 5 ($\Delta x = 0.2810$ Å), and the segment of the line C_β-C_γ equally into 6 ($\Delta x = 0.2370$ Å). Thus, the shape of the mesh was rectangular. The number of the grid points is 46 $\times$ 11 = 506 points for the naphthalene/hydrogen system, and is 46 $\times$ 17 = 782 points for the pyrene/hydrogen system, although the presence of symmetry reduced these numbers to 276 points for the former and 414 points for the latter.

3. Results and Discussion

3.1. Numerical Results. 3.1.1. Naphthalene/Hydrogen and Pyrene/Hydrogen Intermolecular Potential. The intermolecular potential (E(*x*, *z*)) for naphthalene and hydrogen at the MP-2/6-311G* level and that for pyrene and hydrogen at the MP-2/6-31G* level are shown in Figures 3 and 4, respectively.[41] For these calculations, the geometries of naphthalene, pyrene, and the hydrogen molecule were not varied. The horizontal scale showing distance in Figures 3 and 4 is the distance between the plane of the substrate molecule (naphthalene or pyrene) and the hydrogen atom closest to the substrate molecule in the hydrogen molecule. For the naphthalene/hydrogen system at the MP-2/6-311G* level, the lowest energies are obtained at a distance between the molecules of 2.90 Å for the points above α, P_1 and P_2, and 2.95 Å for the points above P_3, P_4 and P_5 (Figure 3). At the MP-2/6-31G* level, the energies are located at a distance of 3.00 Å for the points above α, P_1 and P_2, and 3.05 Å for the points above P_3, P_4 and P_5, giving slightly longer distances than those at the MP-2/6-311G* level.[42−49] For the pyrene/hydrogen system at the MP-2/6-31G* level, the distance is slightly shorter than the distance for the naphthalene/hydrogen system at the same level of calculation: 2.95 Å for points above δ and P_1, 3.00 Å for P_2 and P_3, and 3.05 Å for P_4, P_5, P_6, P_7 and P_8 (Figure 4). These values indicate the presence of a weak tendency of the distance to be longer when the hydrogen molecule becomes closer to the C−C bond from the center of the six-membered ring.

For the naphthalene/hydrogen system at the MP-2/6-311G* level, the energy above point α is the lowest when the distance is less than 1.80 Å, and when the values are compared at the same distance. In the region where the distance is between 1.85 and 2.95 Å, energies above the point P_1 are the lowest. If the distance is longer than 3.00 Å, the point corresponding to the lowest energy moves further out from the center of the six-membered ring. For example, at the distance of 3.65 Å, the energy above the point P_5 is the lowest, although we note that in the region where the distance is longer than 3.00 Å, the potential curve along the x-axis is essentially isoenergetic with the difference between maximum and minimum energies being less than 1.0×10^{-3} eV. Note that in the region where the distance is less than 3.00 Å, energies above the point P_5 are the highest.

Contrary to the results at the MP-2/6-311G* level, the MP-2/6-31G* calculations predict that energies above point α are always the lowest except in the region of the distance being between 2.70 and 2.85 Å, where the energies for P_1 are the lowest. We note that in the region where the distance is longer than 2.25 Å, energies for the points above α and P_1 are essentially isoenergetic with the difference being less than 5.0×10^{-4} eV. Energies above the point P_6 are, again, the highest, except in the region where the distance is longer than 3.30 Å.

For the pyrene system which is calculated only at the MP-2/6-31G* level, the order of the energies above points δ, P_1, P_2, P_3, P_4, P_5, P_6, P_7, and P_8 is $\delta < P_1 < P_2 < P_3 < P_4 < P_5$ and $P_8 < P_7 < P_6 < P_5$ in the region where the distance is less than 2.95 Å. Thus, the energies above the carbon atom are the highest and the lowest energies are those above the center of the six-membered ring. In the region where the distance is longer than 3.00 Å, the energy difference between the maximum and the minimum is less than about 1.0×10^{-3} eV.

To our knowledge, there has been no theoretical and/or experimental report on intermolecular potentials for the systems of either naphthalene or pyrene and a hydrogen molecule. We note that there is even no report on intermolecular potentials between benzene and a hydrogen molecule. Of course, there has been a great deal of theoretical and experimental studies on the so-called van der Waals molecules.[43] For systems which contain benzene, benzene/rare gas,[47,50,51] benzene/N_2,[52] and the benzene dimers[53] have, for example, been investigated theoretically. According to our calculations for naphthalene, the stabilization energy for the formation of a complex with a hydrogen molecule is calculated to be 0.028 and 0.034 eV at the MP-2/6-31G* and MP-2/6-311G* levels, respectively. For pyrene, this energy is calculated to be 0.031 eV at the MP-2/6-31G* level. For benzene/N_2, the energy calculated at the MP-2/6-31+G* level is reported to be 0.074 eV,[52] and for the

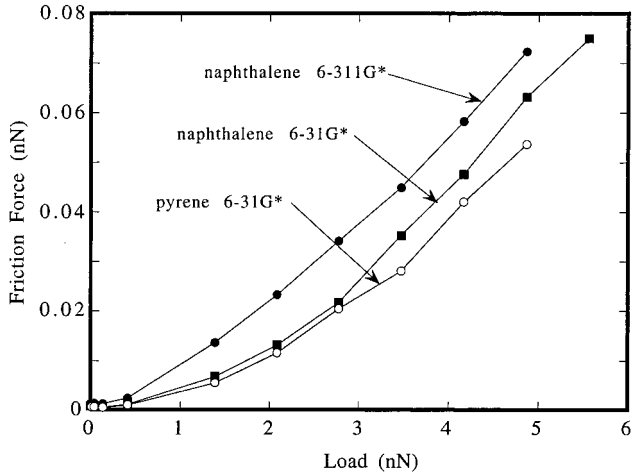

Figure 5. Calculated dependence of friction force on the load.

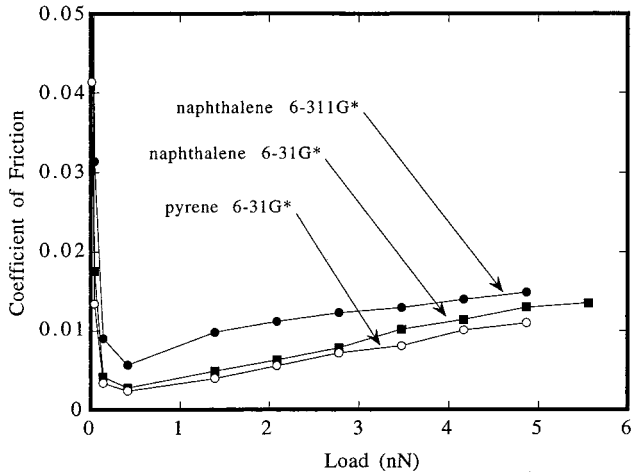

Figure 6. Calculated dependence of friction coefficient on the load.

benzene/Ne complex, the value is calculated to be 0.020 eV at the MP-2/6-311G + diffuse functions level.[47] These reported values show that the order of magnitude for our calculated values does not differ significantly as compared to the values for typical van der Waals complexes.

3.1.2. van der Waals Friction. By using the van der Waals intermolecular potentials obtained, we calculated the friction force and the coefficient of friction. Calculated dependence of friction force (f_f) and the coefficient of friction (μ) on the load (f_N) is shown in Figures 5 and 6, respectively.

For the naphthalene/hydrogen system at the MP-2/6-311G* level, points above α and P_5 give a maximum and minimum value, respectively, in the isopressure potential if $f_N > \sim 0.04$ nN. At the MP-2/6-31G* level for the naphthalene/hydrogen system, the same result was obtained if $f_N > \sim 0.4$ nN. This indicates that if the load is large ($>0.04-0.4$ nN), hill-tops in the isopressure potential are located above the center of a six-membered ring, which is contrary to expectation. If the load is smaller than these values, the maximum and minimum tend to locate at points above P_5 and α, respectively, as is expected and is consistent with the results on the intermolecular potential. For pyrene at the MP-2/6-31G* level, the situation is slightly more complicated. If the load is larger than about 0.4 nN, points above δ and P_8 give a maximum value in the isopressure potential with the energy minimum being above point P_5 or P_6. If the load is smaller than 0.4 nN, the energy maximum tends to appear above point P_5 (i.e., carbon atom) and the minimum above points δ (center of a six-membered ring) and P_8 (center of a C−C bond). These results show that the points corresponding to the maximum and minimum in the isopressure potential when the load is smaller than 0.04−0.4 nN are different from the points when the load is larger than 0.04−0.4 nN.

Calculated values for the naphthalene/hydrogen system at the two levels of MP-2/6-31G* and MP-2/6-311G* do not differ significantly, showing that the basis-set dependence of the calculated values is not significant, and thus we may be able to examine the problem quantitatively. The values for the naphthalene/hydrogen and pyrene/hydrogen systems at the MP-2/6-31G* level are calculated to be essentially the same. This suggests that the friction force and the coefficient of friction is isotropic on the surface of graphite, and does not depend on the direction of motion, although we note that further calculations in which the direction is changed are required to verify this.

As is shown in Figure 5, the friction force increases with an increase in the load. Furthermore, if the load is large enough ($f_N > 3-4$ nN), the friction force becomes almost linear to the load for all systems examined, and consequently, calculated values μ tend to become independent of the load. This indicates that even in the microscale world, Amontons's rule holds essentially true if the load is large enough. In this region, our calculations predict that the coefficient of friction between graphite and hydrogen molecule will be about 0.011−0.015.

In the previous ab initio pseudopotential calculations for the friction between graphite and palladium done by Zhong et al.,[19] the calculated μ was not constant in the region of $f_N > 3-4$ nN, but increased significantly with an increase in the load. For example, their calculated μ at $f_N = 10$ nN was about 0.02 whereas that at $f_N = 30$ nN was about 0.06.[19] This suggests that the presence of chemisorption bonding induces enhanced dependence of the coefficient of friction on the load, as compared to cases where van der Waals interactions are mainly present and thus, Amontons's rule did not hold for their calculations. Furthermore, in this region of $f_N > 3-4$ nN, their calculated values of μ are larger than ours, suggesting that if a strong interaction is present, the magnitude of friction would be enhanced.

In a region where $f_N \sim 0$, the calculated μ become infinite (Figure 6), as our calculations predict that the friction force is still nonzero (1.29×10^{-3} nN at the MP-2/6-311G* level for the naphthalene/hydrogen system) even if $f_N = 0$ nN. If the load becomes zero, the hydrogen molecule moves on the surface of graphite by tracing the energy minimum points in the intermolecular potentials shown in Figures 3 and 4. Even in the trajectory of this motion, energy still has hills and valleys, leading to a nonzero friction force. It should be noted that in the report by Zhong et al.,[19] the coefficient of friction is calculated to be almost zero at $f_N = 0$ nN, in contrast to our results. This is probably because in their calculations, the distance between the two bodies may become infinite at zero-load, due to the lack of van der Waals interactive forces.

3.1.3. Comparison with Experimental Results. Because the calculated values are those for the friction at a molecular or atomic scale, experiments for which direct comparisons can be made are limited to those done by applying the friction force microscopy (FFM) technique. For the purpose of comparison, experimental microscale friction forces and the coefficients of friction of graphite measured by FFM are summarized in Table 1.[12,29,54−56] The values of f_f and f_N in Table 1 cannot directly be compared to our calculated values, as our calculated values for f_f and f_N are normalized by the area corresponding to one hydrogen atom, whereas the experimental values for f_f and f_N apply to the total contact area between graphite or carbonaceous

TABLE 1: Experimental Microscale Friction Forces and Friction Coefficients of Graphite Measured by FFM

carbonaceous material/ tip material	microscale friction force or friction coefficient	load
graphite/tungsten[a]	$\mu = 0.012$	$10^{-6}-10^{-5}$ N
graphite/tungsten[b]	$\mu = 0.01$	$10^{-8}-10^{-6}$ N
graphite/Si_3N_4[c]	$\mu = 0.013$	0−∼150 nN
	$f_f = 7$ nN	0 nN
	$f_f = \sim 8$ nN	∼75 nN
	$f_f = \sim 8.5$ nN	∼115 nN
	$f_f = \sim 9$ nN	∼150 nN
highly oriented pyrolytic graphite/Si_3N_4[d]	$f_f = \sim 0.2$ nN	25 nN
highly oriented pyrolytic graphite/silicon nitride[e]	$\mu = \sim 0.006$	0−∼55 nN

[a] Reference 12. [b] Reference 29. [c] Reference 54. [d] Reference 55. [e] Reference 56.

materials and the end of the FFM tip. Thus, considerable care is required for comparison between the experimental and calculated values for f_f and f_N. To compare f_f and f_N, their values must be normalized, whereas for μ, a direct comparison can be made, as for this quantity, the effect of the difference in the magnitude of contact area is excluded.

For the coefficient of friction, values of 0.012 and 0.01 have been reported for a load ranging from $\sim 10^{-8}$ N to $\sim 10^{-5}$ N by using an FFM tip made of tungsten,[12,29] in excellent agreement with our calculated value of 0.011−0.015, although we note that the tip material is tungsten instead of hydrogen in the calculations. It has been estimated that the applied load in FFM studies is less than 10^{-8} N per atom, because if the magnitude of f_N exceeds this value, strong deformation of graphite is expected, which is in contrast to experiments.[57,58] If we assume that the maximum applied load in the experiments (2×10^{-5} N) corresponds to the load per atom of 10^{-8} N, the contact area becomes in the order of 100 Å × 100 Å.[59] This value is smaller than the experimentally estimated area of contact of about 1000 Å × 1000 Å reported by Mate et al.,[12] which was obtained assuming the tip radius to be about 3000 Å. If we apply the value obtained by Mate et al., the maximum applied load in the experiments can be converted into a value per atom of about 0.01 nN, whereas if the value of the contact area of 100 Å × 100 Å is applied, it becomes 10 nN, revealing the inaccuracy of simple conversion. Considering this inaccuracy, it can be suggested that the range of f_N in Figures 5 and 6 is comparable to the range in the FFM studies of $\sim 10^{-8}$ N to $\sim 10^{-5}$ N.[12,29] We note that this may further support the agreement on μ obtained here.

The dependence of f_f on f_N is actually not exactly linear in the range of f_N from $\sim 10^{-6}$ N to $\sim 10^{-5}$ N, as reported by Mate et al.[12] If we fit Mate's experimental data by the power law against the load, the order becomes about 1.14, slightly larger than unity. This is in qualitative agreement with our calculated result, although quantitatively, our calculated order is 1.32 (naphthalene/hydrogen system at the MP-2/6-311G* level) which is larger than the experimental value.

When the load is smaller, an experimental value of $\mu < 0.006$ at $f_N = 0 - \sim 55$ nN has been reported by Ruan et al. for highly oriented pyrolytic graphite with the use of an FFM tip made of silicon nitride.[56] If we assume that the load per atom also decreases with the decrease in the load for the FFM tip, this experimental result also supports our calculated predictions on μ. As shown in Figure 6, our calculated value decreases with the decrease in load, exhibiting a minimum value of 0.0056 at $f_N = 0.41$ nN at the MP-2/6-311G* level, which is in semiquantitative agreement with the experimental result, although we note again that the tip material in the experiment is silicon nitride instead of hydrogen in the calculations.

In this region of the load, another experimental result is available. Labardi et al.[54] have reported the value of μ in this region to be about 0.013, although they defined μ as df_f/df_N, as they observed a large nonzero f_f (7 nN) at the zero-load, contrary to the other experiments in Table 1. They attributed this large friction force to probable atmospheric contaminants at the interface. However, it is interesting to note that if we convert our f_f per atom at the zero-load by using the area of contact of about 100 Å × 100 Å, f_f per tip becomes about 2 nN, which is in qualitative agreement to the value obtained by Labardi et al., although numerical errors may be large in this region of $f_N \sim 0$ nN.

The other comparison which could be made is that between our numerical values and the macroscale experimental values[60−65] which are listed in Table 2. A typical value of the macroscale coefficient of friction of graphite is about 0.1,[60−65] so that our numerical value is significantly smaller than the macroscale value, as has previously pointed out in the theoretical study by Zhong et al.[19−21] and in experimental studies done using FFM.[12,29,54−56] However, in some experimental studies, much lower macroscale coefficients of friction than 0.1 have been observed under various controlled atmospheres for hard carbon containing hydrogen and polycrystal graphite.[62,65] For these compounds, values of 0.01−0.02 have been obtained. Thus, our theoretical value can be regarded as around the lower limit of the experimental values. This may mean that our calculated μ of 0.011−0.015 corresponds to the first term in eq 2,[15] representing the molecular friction.

3.2. Theoretical Results. To obtain a further insight into the friction phenomena in the microscale world as shown in Figures 5 and 6, we modeled the phenomena theoretically. An

TABLE 2: Experimental Macroscale Friction Coefficients of Graphite

graphite	in ambient air, temperature: 77 ± 3 °F, humidity: 50 ± 1%	0.0593−0.1010[60]
cast iron graphites	air pressure: 10^{-6} to 10^2 mmHg, water vapor pressure: 4−20 mmHg, temperature: 20−140 °C	∼0.12−∼0.35[61]
hard carbon	in air	∼0.1−∼0.3[62]
	in vacuum	∼0.12−∼0.4[62]
hard carbon containing hydrogen	in air	∼0.22−∼0.5[62]
	in vacuum	∼0.01−∼0.35[62]
graphitic carbon	in O_2, pressure: 10^{-1} to 10^2 Torr	∼0.3−∼0.6[63]
graphite	in vacuum	∧0.15[64]
polycrystal graphite	in He (0.4×10^5 Pa)	∼0.02−∼0.45[65]
	in Ar (2×10^5 Pa)	∼0.02−∼0.45[65]
	in He (1×10^5 Pa) and O_2 (1.5×10^5 Pa)	∼0.03−∼0.44[65]

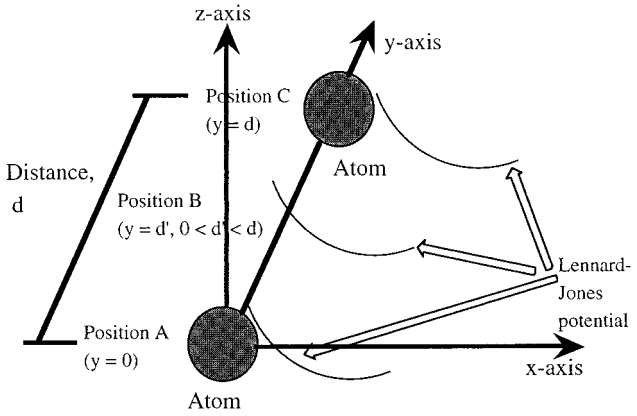

Figure 7. A schematic of the theoretical model. The *yz* plane is the surface of graphite.

assumption that we made is schematically shown in Figure 7. In Figure 7, the surface of a body lies in the *yz* plane, and the other body such as a hydrogen molecule moves along the *y*-direction at $z = 0$. Along this direction, the surface feature is assumed to be periodic with a periodic distance of d. Thus, the interbody potential at $y = 0$ (position A) and at $y = d$ (position C) becomes the same. We assume here that in the interaction potential under a constant load (isopressure potential, $E_f(x)$), the maximum value is at $y = 0$ and d, whereas a minimum value can be seen where $y = d'$ ($0 < d' < d$) (position B). The form of the interaction potential between the two bodies may be represented by the (6,12) potential of Lennard−Jones. Then, the interbody potential at the position A and C can be expressed as

$$V_A(x) = E_A\left\{\left(\frac{C_{1A}}{x}\right)^{12} - \left(\frac{C_{2A}}{x}\right)^{6}\right\} \tag{6}$$

whereas at the position B, it is

$$V_B(x) = E_B\left\{\left(\frac{C_{1B}}{x+R}\right)^{12} - \left(\frac{C_{2B}}{x+R}\right)^{6}\right\} \tag{7}$$

In the region where the distance x is small (which means that the load f_N is large), the second terms in eqs 6 and 7 can be ignored. Using the procedure described above, the microscale friction force and the coefficient of friction in this region were calculated, yielding the following equations.

$$f_f = \left(\frac{1}{12}\right)^{12/13}({E_A}^{1/13}{C_{1A}}^{12/13} - {E_B}^{1/13}{C_{1B}}^{12/13}){f_N}^{12/13}/d \tag{8}$$

$$\mu = \left(\frac{1}{12}\right)^{12/13}({E_A}^{1/13}{C_{1A}}^{12/13} - {E_B}^{1/13}{C_{1B}}^{12/13}){f_N}^{-1/13}/d \tag{9}$$

The general form of the Lennard−Jones potential is known to be in the form of

$$V(x) = \frac{C_n}{x^n} - \frac{C_m}{x^m} \tag{10}$$

where x is the distance, and C_n and C_m are constants.[66] Thus, eqs 8 and 9 would further be generalized by assuming the shape of the interbody potentials to be proportional to $(1/x)^n$ instead of to $(1/x)^{12}$ at position A, and at position B, to $(1/x)^{n'}$, as the exponent at position B may be different from that at position A. In this case, the two equations become

$$f_f = \left\{\left(\frac{1}{n}\right)^{n/(n+1)}{E_A}^{1/(n+1)}{C_{1A}}^{n/(n+1)}{f_N}^{n/(n+1)} - \left(\frac{1}{n'}\right)^{n'/(n+1)}{E_B}^{1/(n'+1)}{C_{1B}}^{n'/(n'+1)}{f_N}^{n'/(n'+1)}\right\}/d \tag{11}$$

$$\mu = \left\{\left(\frac{1}{n}\right)^{n/(n+1)}{E_A}^{1/(n+1)}{C_{1A}}^{n/(n+1)}{f_N}^{-1/(n+1)} - \left(\frac{1}{n'}\right)^{n'/(n'+1)}{E_B}^{1/(n'+1)}{C_{1B}}^{n'/(n'+1)}{f_N}^{-1/(n'+1)}\right\}/d \tag{12}$$

In the region of x where the (6,12) potentials are around the minimum, eqs 6 and 7 may be approximated by a parabolic form, so that the two equations can be expressed as

$$V_A(x) = E'_A(x - R'_A)^2 + E''_A \tag{13}$$

$$V_B(x) = E'_B(x - R'_B)^2 + E''_B \tag{14}$$

The friction force and the coefficient of friction can then be calculated as,

$$f_f = \left\{\left(\frac{1}{4E'_A} - \frac{1}{4E'_B}\right)f_N^2 + E''_A - E''_B\right\}/d \tag{15}$$

$$\mu = \left\{\left(\frac{1}{4E'_A} - \frac{1}{4E'_B}\right)f_N + \frac{E''_A - E''_B}{f_N}\right\}/d \tag{16}$$

Finally, in the region where x is large, where the interbody van der Waals force becomes attractive, the first terms in eqs 6 and 7 can be ignored. Then, the microscale friction force and the coefficient of friction can be expressed as

$$f_f = \left(\frac{1}{6}\right)^{6/7}(-{E_A}^{1/7}{C_{2A}}^{6/7} + {E_B}^{1/7}{C_{1B}}^{6/7})(-f_N)^{6/7}/d \tag{17}$$

$$\mu = \left(\frac{1}{6}\right)^{6/7}(-{E_A}^{1/7}{C_{2A}}^{6/7} + {E_B}^{1/7}{C_{1B}}^{6/7})(-f_N)^{-1/7}/d \tag{18}$$

The negative sign of f_N in eqs 17 and 18 shows that the direction of the load is opposite from that in the case in which the load f_N is large, because in this region the interbody force is attractive. A similar generalization to that which gave eqs 11 and 12 can be made by assuming that the interbody potentials can be described in the form shown in eq 10 instead of eqs 6 and 7. The shape of the interbody potential, then, becomes proportional to $(1/x)^m$ instead of to $(1/x)^6$ at position A, and to $(1/x)^{m'}$ at position B. This yields the two equations below.

$$f_f = \left\{-\left(\frac{1}{m}\right)^{m/(m+1)}{E_A}^{1/(m+1)}{C_{2A}}^{m/(m+1)}(-f_N)^{m/(m+1)} + \left(\frac{1}{m'}\right)^{m'/(m'+1)}{E_B}^{1/(m'+1)}{C_{2B}}^{m'/(m'+1)}(-f_N)^{m'/(m'+1)}\right\}/d \tag{19}$$

$$\mu = \left\{\left(\frac{1}{m}\right)^{m/(m+1)}{E_A}^{1/(m+1)}{C_{2A}}^{m/(m+1)}(-f_N)^{-1/(m+1)} - \left(\frac{1}{m'}\right)^{m'/(m'+1)}{E_B}^{1/(m'+1)}{C_{2B}}^{m'/(m'+1)}(-f_N)^{-1/(m'+1)}\right\}/d \tag{20}$$

These equations give the dependence of the microscale friction force and the coefficient of friction on the load, as is schematically shown in Figures 8 and 9. For f_f, it is calculated that in the region where the interbody distance is large (or the load is negative), the magnitude of the force is proportional to $|f_N|^{6/7}$ (or $|f_N|^{m/(m+1)} - |f_N|^{m'/(m'+1)}$), and becomes larger with an increase in $|f_N|$. In this region where f_N is negative or the interbody force is attractive, the magnitude of the load cannot become larger than a certain value which is limited by the

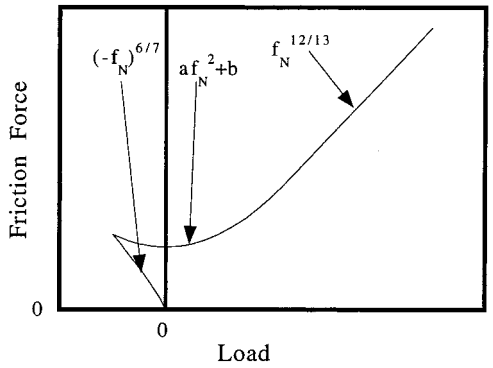

Figure 8. Schematic showing dependence of microscope friction force on load.

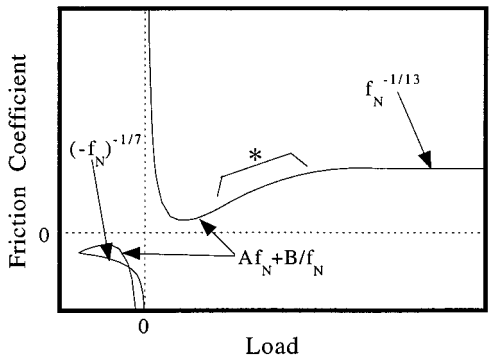

Figure 9. Schematic showing dependence of microscope friction coefficient on load.

maximum of the gradient of the interbody van der Waals potential in the attractive force region. In the intermediate region where the two bodies are almost put into contact by the van der Waals attractive force, the dependence of the friction force on the load is calculated to be parabolic, with the magnitude of the friction force increasing with an increase in the absolute value of the load. We note that f_f is not zero even if f_N is zero. Finally, in the region where the interbody distance is small and where the van der Waals repulsive force operates, the magnitude of the friction force is calculated to be proportional to $|f_N|^{12/13}$ (or $|f_N|^{n/n+1} - |f_N|^{n'/(n'+1)}$), or if $n = n'$, the friction force becomes to be proportional to $f_N^{n/(n+1)}$, becoming almost linear with f_N.

For μ, the negative coefficient is calculated in Figure 9 in the region where the interbody distance is large (or the load is negative), because the sign of the load is negative in this region, whereas the friction force is always positive because its direction does not change. In this region, the coefficient of friction is calculated to be proportional to $|f_N|^{-1/7}$ (or $|f_N|^{-1/(m+1)} - |f_N|^{-1/(m'+1)}$). In the region where two bodies are put into contact by the van der Waals attractive force, the coefficient of friction is in the form of $A \times f_N + B/f_N$ (A and B are constants). Thus, as can be seen in Figure 9, in the van der Waals repulsive force region, the coefficient of friction at zero-load is infinite, and then it decreases at first, and then increases linearly with the increase in the load. Subsequently, the coefficient becomes proportional to $|f_N|^{-1/13}$ (or $|f_N|^{-1/(n+1)} - |f_N|^{-1/(n'+1)}$) in the region where the load is large, eventually showing a local maximum value.

Comparing Figures 5 and 6 to Figures 8 and 9, it can be seen that our theoretical results are qualitatively in agreement with the numerical results. Comparison of the above equations with the numerically calculated values is done for the numerical results of the naphthalene/hydrogen system at the MP-2/6-311G* level. The interbody potentials shown in Figure 3 over points

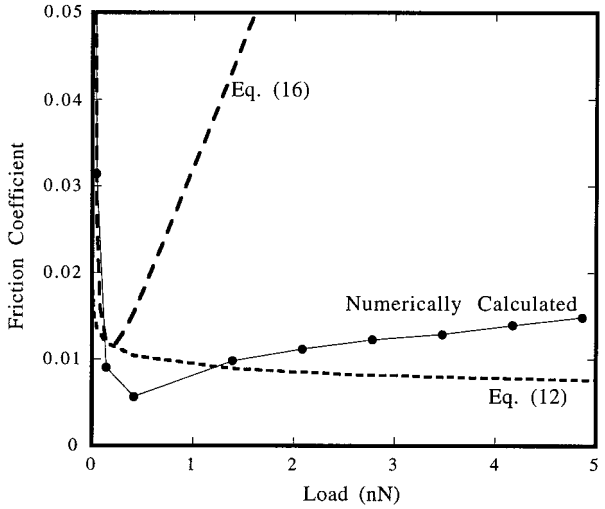

Figure 10. Numerically and theoretically calculated friction coefficient for the naphthalene/hydrogen system at the MP-2/6-311G* level.

α and P_5 are fitted by eqs 6 and 7 or eqs 13 and 14,[67] and the constants obtained are substituted into eqs 12 and 16 for the coefficient of friction. Values for μ are shown in Figure 10 for eqs 12 and 16, where the former is for the region where f_N is sufficiently large, and the latter for $f_N \sim 0$. We note that for calculating eq 12, the interbody potentials at points above α and P_5 (Figure 3) are not actually fitted by eqs 6 and 7 but are fitted by a function having a form which is more generalized than that of eqs 6 and 7, as shown in eq 21.[68]

$$V(x) = E\left\{\left(\frac{C_1}{x+R}\right)^n - \left(\frac{C_2}{x+R'}\right)^m\right\} \qquad (21)$$

Figure 10 shows that the theoretical curve for $f_N = \sim 0$ (eq 16) agrees with the numerically calculated values if $f_N < \sim 0.1$ nN,[69] whereas in the region where f_N is large ($f_N > \sim 1$ nN), the theoretical curve from eq 12 does not show a tendency similar to the numerical results.[70] In this region, the numerically calculated value increases with an increase in the load, whereas in the curve from eq 12, the theoretical value decreases. As has been discussed in the comparison between the numerical and experimental results, the power low for the microscale friction force against the load exceeds unity which is contrary to eq 8 and eq 11. This indicates that this region of $f_N = 0.5-5$ nN (or more) can be regarded as an intermediate region between those which can be described by eq 17 and eq 12, and corresponds to the region which is marked by an asterisk in Figure 9.

4. Conclusions

Ab initio molecular orbital calculations predict the coefficient of friction of graphite in microscale to be 0.011−0.015 for model systems of a naphthalene/hydrogen molecule and a pyrene/hydrogen molecule. This value is in excellent agreement with various friction force microscope measurements and is located in the lower limit of the varied macroscale values. On the other hand, this value is smaller than the previously reported numerical value for friction between graphite and palladium, showing that the presence of chemisorption bonding may enhance the magnitude of friction. A simple theoretical model to describe the numerically calculated dependence of the microscale friction force and the coefficient of friction on the load is also formulated. This theoretical result is in qualitative agreement with the numerical results.

Acknowledgment. The authors would like to acknowledge Dr. Jun′etsu Seto, Dr. Haruo Watanabe, Mr. Hidemi Tomita, and Mr. Takahiro Kamei for their useful discussions.

References and Notes

(1) Amontons, G. *Hist. Acad. R. Soc., Paris* **1699**, *12*, 206.
(2) Coulomb, E. *Mem. Math. Phys., Paris* **1785**, *10*, 161.
(3) Halling, J. *Principles of Tribology*; The Macmillan Press: U. K., 1975.
(4) *Friction, Wear and Lubrication*; Kragelsky, I. V., Alisin, V. V., Eds.; Mir Publishers: Moscow, 1978.
(5) Czichos, H. *Tribology*; Elsevier: Amsterdam, 1978.
(6) Iliuc, I. *Tribology of Thin Layers*; Elsevier: Amsterdam, 1980.
(7) *Tribology and Mechanics of Magnetic Storage Devices*; Bhushan, B., Ed.; Springer-Verlag: New York, 1990.
(8) *Surface Diagnostics in Tribology*; Miyoshi, K., Chung, Y. W., Eds.; World Scientific: Singapore, 1993.
(9) Singer, I. L. *J. Vac. Sci. Technol. A* **1994**, *12*, 2605.
(10) Binnig, G.; Quate, C. F.; Gerber, Ch. *Phys. Rev. Lett.* **1986**, *56*, 930.
(11) Binnig, G.; Gerber, Ch.; Stoll, E.; Albrecht, T. R.; Quate, C. F. *Europhys. Lett.* **1987**, *3*, 1281.
(12) Mate, C. M.; McClelland, G. M.; Erlandsson, R.; Chiang, S. *Phys. Rev. Lett.* **1987**, *59*, 1942.
(13) Erlandsson, R.; Hadziioannou, G.; Mate, C. M.; McClelland, G. M.; Chiang, S. *J. Chem. Phys.* **1988**, *89*, 5190.
(14) Meyer, G.; Amer, N. M. *Appl. Phys. Lett.* **1990**, *57*, 2089.
(15) Mikhin, N. M. In *Friction, Wear and Lubrication Vol. 1*; Kragelsky, I. V., Alisin, V. V., Eds.; Mir Publishers: Moscow, 1978; p 54.
(16) Tomlinson, G. A. *Philos. Magn. S* **1929**, *7*, 905.
(17) Frenkel, Y. I.; Kontorova, T. *Zh. Eksp. Teor. Fiz.* **1938**, *8*, 1340.
(18) McClelland, G. M. In *Adhesion and Friction, Springer Series of Surface Sciences, Vol. 17*; Grunze, M., Kreuzer, H. J., Eds.; Springer-Verlag: Berlin, 1989; p 1.
(19) Zhong, W.; Tománek, D. *Phys. Rev. Lett.* **1990**, *64*, 3054.
(20) Overney, G.; Zhong, W.; Tománek, D. *J. Vac. Sci. Technol. B* **1991**, *9*, 479.
(21) Tománek, D.; Zhong, W.; Thomas, H. *Europhys. Lett.* **1991**, *15*, 887.
(22) Overney, R. M.; Meyer, E.; Frommer, J.; Brodbeck, D.; Lüthi, R.; Howald, L.; Güntherodt, H.-J.; Fujihira, M.; Takano, H.; Gotoh, Y. *Nature* **1992**, *359*, 133.
(23) Meyer, E.; Overney, R. M.; Brodbeck, D.; Howald, L.; Lüthi, R.; Frommer, J.; Güntherodt, H.-J. *Phys. Rev. Lett.* **1992**, *69*, 1777.
(24) O'Shea, S. J.; Welland, M. E.; Rayment, T. *Appl. Phys. Lett.* **1992**, *61*, 2240.
(25) Hipp, M.; Bielefeldt, H.; Colchero, J.; Marti, O.; Mlynek, J. *Ultramicroscopy* **1992**, *42*−*44*, 1498.
(26) O'Shea, S. J.; Welland, M. E.; Wong, T. M. H. *Ultramicroscopy* **1993**, *52*, 55.
(27) O'Shea, S. J.; Welland, M. E.; Rayment, T. *Langmuir* **1993**, *9*, 1826.
(28) Haugstad, G.; Gladfelter, W. L.; Weberg, E. B. *Langmuir* **1993**, *9*, 3717.
(29) Mate, C. M. *Wear* **1993**, *168*, 17.
(30) Gaussian 94, Revision B.3; Frisch, M. J.; Trucks, G. W.; Schlegel, H. B.; Gill, P. M. W.; Johnson, B. G.; Robb, M. A.; Cheeseman, J. R.; Keith, T.; Petersson, G. A.; Montgomery, J. A.; Raghavachari, K.; Al-Laham, M. A.; Zakrzewski, V. G.; Ortiz, J. V.; Foresman, J. B.; Peng, C. Y.; Ayala, P. Y.; Chen, W.; Wong, M. W.; Andres, J. L.; Replogle, E. S.; Gomperts, R.; Martin, R. L.; Fox, D. J.; Binkley, J. S.; Defrees, D. J.; Baker, J.; Stewart, J. P.; Head-Gordon, M.; Gonzalez, C.; Pople, J. A.; Gaussian, Inc., Pittsburgh PA, 1995.
(31) Ditchfield, R.; Hehre, W. J.; Pople, J. A. *J. Chem. Phys.* **1971**, *54*, 724.
(32) Hehre, W. J.; Ditchfield, R.; Pople, J. A. *J. Chem. Phys.* **1972**, *56*, 2257.
(33) Hariharan, P. C.; Pople, J. A. *Mol. Phys.* **1974**, *27*, 209.
(34) Gordon, M. S. *Chem. Phys. Lett.* **1980**, *76*, 163.
(35) Hariharan, P. C.; Pople, J. A. *Theor. Chim. Acta* **1973**, *28*, 213.
(36) McLean, A. D.; Chandler, G. S. *J. Chem. Phys.* **1980**, *72*, 650.
(37) Krishnan, R.; Binkley, J. S.; Seeger, R.; Pople, J. A. *J. Chem. Phys.* **1980**, *72*, 650.
(38) Møller, C.; Plesset, M. S. *Phys. Rev.* **1934**, *46*, 618.
(39) The points α and γ are defined as the center of the segment of the line $C_\alpha-C_\delta$ and $C_\epsilon-C_\zeta$, respectively.
(40) The points δ and ϵ are defined as the center of the segment of the line $C_\alpha-C_\beta$ and $C_\gamma-C_\delta$, respectively.
(41) This intermolecular potential was calculated as $E(x, z) = E$(naphthalene or pyrene/hydrogen molecule) − E(naphthalene or pyrene) − E(hydrogen molecule). Calculated energy for naphthalene was −384.61465476981 Ha and −384.73786470882 Ha at the MP-2/6-31G* and MP-2/6-311G* level, respectively. For pyrene, the energy was −613.78733125643 Ha at the MP-2/6-31G* level, and for the hydrogen molecule, the value was −1.1441408483251 Ha at MP-2/6-31G*, and −1.1458815873186 Ha at MP-2/6-311G*.
(42) We note that a similar basis set dependence has been calculated in many reports for various molecular systems. See, for example, refs 43−49.
(43) *Chem. Rev. (Washington, D.C.)* **1994**, *94*, 4, No. 7.
(44) Amos, R. D.; Handy, N. C.; Knowles, P. J.; Rice, J. E.; Stone, A. J. *J. Phys. Chem.* **1985**, *89*, 2186.
(45) Matías, M.; Tel, L. M.; Novoa, J. J. *J. Comput. Chem.* **1987**, *8*, 51.
(46) Bone, R. G. A.; Handy, N. C. *Theor. Chim. Acta* **1990**, *78*, 133.
(47) Brupbacher, Th.; Lüthi, H. P.; Bauder, A. *Chem. Phys. Lett.* **1992**, *195*, 482.
(48) Antonio, J.; Romero, M.; Sanz, J. F. *J. Mol. Struct.* **1993**, *287*, 149.
(49) Yin, D.; MacKarell, A. D., Jr. *J. Phys. Chem.* **1996**, *100*, 2588.
(50) Hobza, P.; Selzle, H. L.; Schlag, E. W. *J. Chem. Phys.* **1991**, *95*, 391.
(51) Hobza, P.; Bludsky, O.; Selzle, H. L.; Schlag, E. W. *J. Chem. Phys.* **1992**, *97*, 335.
(52) Hobza, P.; Bludsky, O.; Selzle, H. L.; Schlag, E. W. *J. Chem. Phys.* **1993**, *98*, 6223.
(53) Hobza, P.; Selzle, H. L.; Schlag, E. W. *J. Chem. Phys.* **1990**, *93*, 5893.
(54) Labardi, M.; Allegrini, M.; Salerno, M.; Frediani, C.; Ascoli, C. *Appl. Phys. A* **1994**, *59*, 5.
(55) Ruan, J.-A.; Bhushan, B. *J. Appl. Phys.* **1994**, *76*, 5022.
(56) Ruan, J.-A.; Bhushan, B. *J. Tribol.* **1994**, *116*, 378.
(57) Tománek, D.; Overney, G.; Miyazaki, H.; Mahanti, S. D.; Güntherodt, H. J. *Phys. Rev. Lett.* **1989**, *63*, 876.
(58) Mamin, H. J.; Ganz, E.; Abraham, D. W.; Thomson, R. E.; Clarke, J. *Phys. Rev. B* **1986**, *34*, 9015.
(59) Here, we assume the area corresponding to one atom to be 2.4 Å × 2.4 Å (Note that the van der Waals' radius of hydrogen atom is 1.2 Å (*CRC Handbook of Chemistry and Physics*, 64th ed.; Weast, R. C., Astle, M. J., Beyer, W. H., Eds.; CRC Press: Boca Raton, FL, 1984; p D-191).
(60) Whitehouse, G. D.; Nandan, D.; Whitehurst, C. A. *ASLE Trans.* **1970**, *13*, 159.
(61) Sugishita, J.; Fujiyoshi, S. *Wear* **1981**, *68*, 7.
(62) Miyake, S.; Takahashi, S.; Watanabe, I.; Yoshihara, H. *ASLE Trans.* **1987**, *30*, 121.
(63) Zaïdi, H.; Paulmier, D.; Lepage, J. *Appl. Surface Sci.* **1990**, *44*, 221.
(64) Zaïdi, H.; Paulmier, D.; Jeanmaire, A.; Néry, H. *Surface Sci.* **1991**, *251/252*, 778.
(65) Zaïdi, H.; Robert, F.; Paulmier, D.; Néry, H. *Appl. Surface Sci.* **1993**, *70/71*, 103.
(66) For example, *American Institute of Physics Handbook*; Gray, E. E., Ed., McGraw-Hill Book Co.: New York, 1963; pp 4−160.
(67) For the fitting by eqs 13 and 14, fitting is done for numerical points between 1.70 Å to 2.75 Å in Figure 3. At the position of α, the fitting yields values of $E'_\alpha = 0.62466$, $R_\alpha = 2.5791$, and $E''_\alpha = -0.035533$, and at the position of P_5, the values are $E'_{P5} = 0.89942$, $R_{P5} = 2.5701$, and $E''_{P5} = -0.037207$, if the units of load, energy, and length are in eV/Å, eV, and Å, respectively.
(68) At the position of α, the fitting yields values of $n = 5.008$, $R = 0.4162$, $E \times C_1^n = 112.81$, $m = -3.480$, $R' = -0.0870$, and $E \times C_2^m = 11.47$, and at the position of P_5, the values are $n = 4.952$, $R = 0.2846$, $E \times C_1^n = 79.86$, $m = -3.141$, $R' = -0.2728$, and $E \times C_2^m = 6.11$, if the units of load, energy, and length are in eV/Å, eV, and Å, respectively.
(69) In the numerical calculations where the load is less than ∼0.1 nN, the distance between naphthalene and hydrogen is in the range of 2.30−2.94 Å located in the region around the minimum of the interbody potentials (the minimum is at ∼2.9 Å, see Figure 3).
(70) In the numerical calculations at the large magnitude of load ($f_N >$ ∼1 nN), the distance between naphthalene and hydrogen is, for example, in a range of 1.45−1.61 Å at $f_N = 4.8$ nN.